Front. Electr. Electron. Eng. China 2009, 4(2): 214–219
DOI 10.1007/s11460-009-0028-8

RESEARCH ARTICLE

Gang WU, Huiling WANG, Jiangbo XIE, Yan ZHAO, Yuejin TANG, Jindong LI, Jing SHI

Loading experiment and thermal analysis for conduction cooled magnet of SMES system

© Higher Education Press and Springer-Verlag 2009

Abstract China's first 35 kJ high temperature superconducting magnetic energy storage (SMES) system with an experiment equipment was depicted. The dynamic heat analysis of the magnet of the SMES was conducted through the current load test on the directly cooled conduction magnet. The research results were as follows: when the converter charges and discharges the magnet for energy storage, the hysteresis loss is the main part of power loss, and contributes significantly to temperature rise; reducing the current frequency at the side of direct current is conducive to restraining temperature rise. The optimizing factors of the cool-guide structure were analyzed based on the heat stability theory, and it was found that the heat transfer of its key part (at the top of the magnet) must be strengthened to reduce the axial temperature difference of the magnet.

Keywords conduction cooled, superconducting magnetic energy storage (SMES) magnet, current load, thermal analysis

1 Introduction

Superconducting magnetic energy storage (SMES) devices utilize a superconducting coil to store energy and achieve high efficiency. Moreover, the SMES can respond very rapidly to exchange active and reactive power independently in four quadrants with an alternating current (AC) power grid connected. With the characteristics above, the SMES system adapts to the load variation, increases transmission capacity and improves the stability of the power system.

The thermal stability of the magnet is extremely significant in the operation of the SMES device [1]. Large temperature rise would result in quenching of the magnet, and thus the thermal analysis, especially the dynamic analysis of the magnet is important in the research and application of the SMES.

2 Configuration of high temperature superconducting magnet

The 35 kJ SMES magnet consists of 32 double pancake coils fabricated with superconducting Bi_{2223} tape with a length of 7399 m. It is about 200 kg in weight and 364.88 mm high. The outside and inside diameters of the high temperature superconducting (HTS) magnet are 272 mm and 150 mm, respectively. There are 31 joints in the magnet. The room temperature resistance of the magnet is about 128 Ω, with the critical voltage of 645 mV (1 μV/cm criterion). The designed current and operating temperature are 100 A and 20–40 K, respectively.

The 35 kJ SMES magnet is directly cooled by a cryocooler, in other words, the cooling power of the G-M cryocooler is conducted to the magnet through the cooling frame which includes conducting poles, upper and lower conducting boards of the magnet, conducting copper flakes and flexible conducting components, etc. The copper conducting poles connect the upper and lower conducting boards and several conducting flakes; flexible conducting components connect down conducting board and the cooling head of the G-M cryocooler A (Fig. 1). A little amount of pure indium is placed on the interface for tight contact. The reciprocating movement of the piston in the G-M cryocooler causes the vibration of the cooling head, which could damage the magnet and affect its stability. Therefore, flexible conducting parts are used to transport the cooling power to the magnet. Meanwhile, the

Translated from *Journal of Huazhong University of Science and Technology* (*Nature Science Edition*), 2007, 35(4): 85–88 [译自: 华中科技大学学报 (自然科学版)]

Gang WU (✉), Huiling WANG, Jiangbo XIE, Yan ZHAO, Yuejin TANG, Jindong LI, Jing SHI
Research Institute of Cryogenics, Huazhong University of Science and Technology, Wuhan 430074, China
E-mail: Wu_G77@tom.com

Gang WU
Department of Mechanical Engineering, Naval University of Engineering, Wuhan 430033, China

conducting rods and flakes ensure every part of the magnet obtains approximately an equal quantity of cooling power and effectively prevent the magnet from local quench. A high purity copper conduction canister is placed in the inner part of the copper framework to intensify the heat transfer and minimize axial temperature difference.

The device possesses two G-M cryocoolers. Cryocooler A is for cooling the magnet and B is for cooling the radiating shield and current leads. The basic setup is shown in Fig. 1.

3 Heat load of HTS magnet

The 35 kJ SMES magnet operates below approximately 20 K temperature through conduction cooling. During charging and discharging, AC loss is produced. Variation of magnetic field with time $\partial B/\partial t$ generates the hysteresis loss in the superconductor and eddy loss in the basis metal of the composite. Besides, current variation $\partial I/\partial t$ produces some self-field loss. All these energy losses are transformed into heat leading to temperature rise of the magnet and great load increment of the cryocooler.

Because of the high vacuum environment around the superconducting magnet work, convection heat transfer could be ignored. The main causes of temperature rise are:

1) AC loss of the magnet.

2) Radiating heat.

3) Heat production in the process of magnet quench [2,3].

3.1 AC loss power of magnet

Hysteresis loss: the magnetic energy storage device undergoes an alternating magnetic field in the process of magnet excitation or discharge. By applying Bean model [4] the average loss of unit length of the superconducting tape is

$$W = 4f\mu_0 bdH^* H_{\mathrm{m}}\left(1+\frac{I_{\mathrm{tm}}^2}{I_{\mathrm{c}}^2}\right), \tag{1}$$

where f is the frequency of the magnetic field, μ_0 is the coefficient of the vacuum magnet conduction, b is the width of the tape, d is half the thickness of the tape, H^* is intension of the outer magnetic field, H_{m} is the peak value of the magnetic field, I_{tm} is the operating current, and I_{c} is the critical current. The quantity of hysteresis loss is mainly concerned with frequency and magnetic field amplitude.

Eddy loss: eddy loss will be generated in the matrix of the composite conductor. In a sinusoidal magnetic field, the unit volume eddy loss is

$$Q_1 = \frac{B^2}{4\mu_0\tau}\left(1+\frac{1}{\omega^2\tau^2}\right)^{-1}, \tag{2}$$

where B is density of magnetic flux, ω is angle frequency, τ is decay time constant of the induced current.

Self-field loss: the change of transporting current leads to the change of self-field which causes movement of flux and generates energy loss. The unit volume self-field loss is [5]

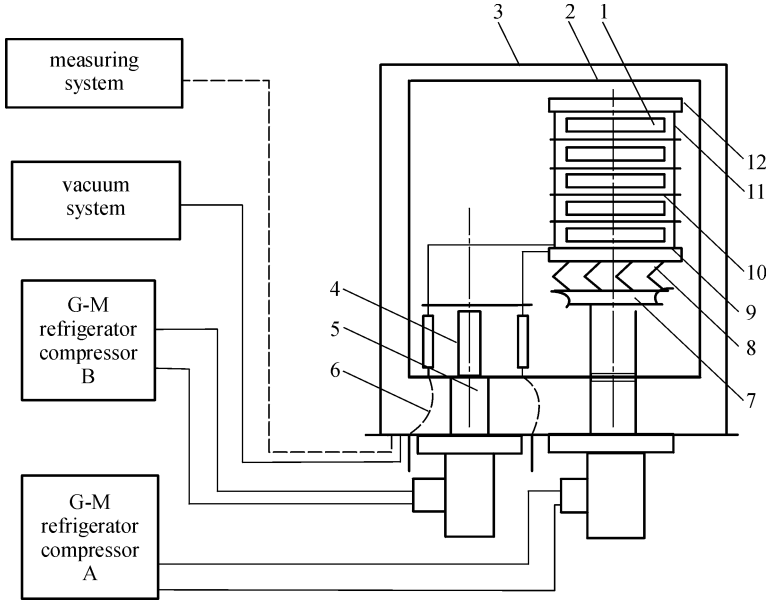

Fig. 1 Conduction cooling system of SMES (1. magnet, 2. radiating shield, 3. cryostat, 4. second stage cooling head of cryocooler B, 5. first stage cooling head of cryocooler B, 6. binary current lead, 7. cooling head of cryocooler A, 8. flexible conducting frame, 9. down conducting board, 10. conducting copper flakes, 11. conducting rods, 12. upper conducting board)

$$Q_2 = \mu_0 \frac{D^2 J^2}{192} \left(\frac{\Delta I}{I_c} \right)^3, \quad (3)$$

where D is the diameter of the composite conductor, J is the average current density, ΔI is the current difference between the minimal and the maximal values.

3.2 Radiating heat

The magnetic energy storage device runs under the constant pressure of 10^{-3} Pa, thus the remaining gas is little. The major extra heat load comes from radiating heat leakage between the magnet and the shield:

$$Q_3 = F\sigma\varepsilon(T_2^4 - T_1^4). \quad (4)$$

In the equation above, F is the magnet external area, σ is Boltzmann constant: $\sigma = 5.67 \times 10^{-8}$ W/(m^2·K^4), ε is black degree of the magnet and the value is 1. T_1, T_2 respectively are the magnet and the shield temperature. To reduce the magnet temperature, the temperature of the shield should be as low as possible.

3.3 Heat load in process of magnet quenching

With an amount of storage energy of the magnet, part of the storage energy would be transformed into heat load in the process of magnet quenching and cause the rise of magnet temperature [6].

3.4 Total heat loads and cooling power of cryocooler

The epoxy plank of the heat insulation is inserted between the magnet and the mechanical support. The heat leak of the current lead is borne by a two-stage G-M cryocooler B, whose cooling power and consumption power are 5.4 W/10 K, 80 W/75 K and 7.5 kW, respectively. For this reason, the thermal performance of the magnet is slightly affected by heat leak of the current leads and mechanical supports.

The temperatures of the magnet and the radiating shield are 25 K and 140 K respectively during the specific operation. The radiating heat leakage is 1.2 W. The AC loss of the magnet is approximately 24 W. The Joule heat of joints is 0.3 W. The eddy loss is about 0.059 W. The total heat loads of the magnet are around 25.6 W. Then we prepared a single stage G-M cryocooler A with a cooling capacity of 58 W at 25 K (consumption power is 7.5 kW).

4 Electric current loading experiment of magnet

The dynamic simulation experiment for SMES is carried out to evaluate the capability of the SMES in compensating the unbalanced power of the AC system. When the fault of line to ground is simulated at the output of the generator, the SMES can deliver or absorb the active power to damp the oscillation of the power system and improve its stability. It is necessary to measure the parameters of the magnet insulation, electric resistance and inductance, and test the current carrying capacity of the magnet before the dynamic experiment.

4.1 Experiment equipment

Cryogenic system: the system mainly consists of a cryostat, radiating shield, conducting strap, conduction cooling board of magnet, conducting flakes, conducting rods, flexible conducting frame, conducting board of cooling head, cryocooler A, and cryocooler B (being shown in Fig. 2).

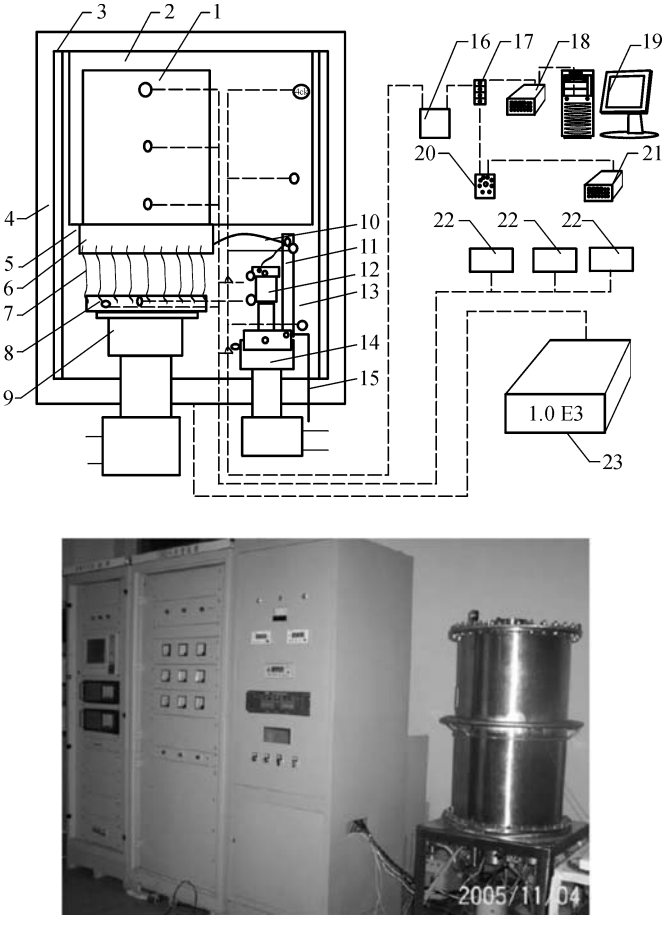

Fig. 2 Cryogenic measuring system of SMES (1. magnet, 2 & 3. radiating shield, 4. cryostat, 5 & 13. conduction strap of radiating shield, 6. magnet down conducting board, 7. flexible conducting frame, 8. cooling head conducting board, 9. cooling head of cryocooler A, 10. current lead, 11 & 15. binary current leads, 12. second stage cooling head of cryocooler B , 14. first stage cooling head of cryocooler B, 16. ice-barrel, 17. connection points, 18. digital temperature receiver, 19. computer, 20. switch, 21. digital voltage receiver, 22. digital temperature display instrument, 23. vacuum instrument)

Vacuum system: the system comprises double stage circumrotating vacuum pump and vacuum instruments that measure the vacuum degree.

Electric current loading system: the system mainly consists of constant current source used in the direct current (DC) loading experiment and multi-module converter employed in the dynamic characteristics experiment.

Temperature measurement: a total of 12 temperature sensors are placed in the magnet, current leads, radiation shield and the cooling head of cryocoolers. The locations of sensors are shown in Fig.2. The types of the sensors include Pt100 electric resistance, NiCr-CuFe and copper-constantan thermal couple. The Pt100 and copper-constantan sensors are used to detect the temperature of current leads and radiation shield. The specially-designed sensor NiCr-CuFe is applied to detect the temperature of the magnet. The measuring results of Pt100 sensors are displayed by a digital instrument; meanwhile, the data together with the results from thermal couple sensors are sent to a computer by the data acquisition system.

Measuring the pressure in the cryostat: the vacuum gauge pipe is set in the base of the cryostat, and a ZDF vacuum instrument is applied to inspect the vacuum degree in the process of operation.

Measurement in the process of current loading: Keithley 2700 data collecting system is applied to measure and record the parameters in DC and dynamic loading experiment.

4.2 Test of HTS magnet

Current loading experiment at liquid nitrogen: the magnet is tested in liquid nitrogen of 77 K before it is strengthened by epoxy. It generates 0.68 T magnetic field when 22 A DC current is loaded. While the 100 A DC current is loaded at lower temperature, the center magnetic field is 3.17 T and the maximal field is 3.28 T. The measurement result reveals that maximal field intensity exists in the 5th and the 32nd coils, it is therefore obvious that the upper part of the magnet is easy to quench when it undergoes thermal disturbance.

Cooldown experiment of magnet and analysis: the pressure of the system is reduced to 0.1 Pa by a vacuum pump before the G-M cryocooler starts; then by the cryocooler the system pressure is continually reduced until around 10^{-3} Pa. The HTS magnet is cooled down to 19 K after 24 hours, and the lowest temperature in the magnet is about 13.5 K. The curve of the cooldown is shown in Fig. 3.

At the beginning, the temperature of the magnet underside is relatively high because the cryocooler mainly cools the flexible conducting frame and the bottom conducting board. Along with the cooling process, the magnet underside starts to turn cool and then the magnet upside follows, thus the temperature difference between the two parts becomes larger, reaching 75 K after 6.5 hours. In the following period, the temperature difference reduces

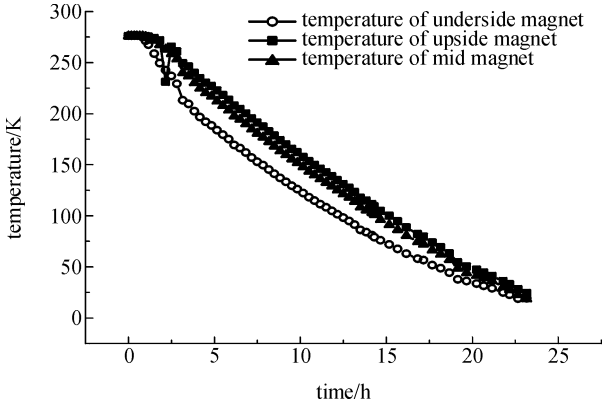

Fig. 3 Cooldown curves of magnet

and tends to balance. After 24 hours, the upside and underside sensors located in the magnet indicate that the temperature difference is just 0.4 K. The slight axial temperature difference reveals that the conducting configuration can equably transport the heat load into the cryocooler in time. The pancakes of the magnet reaching superconducting state are illustrated in Fig. 4.

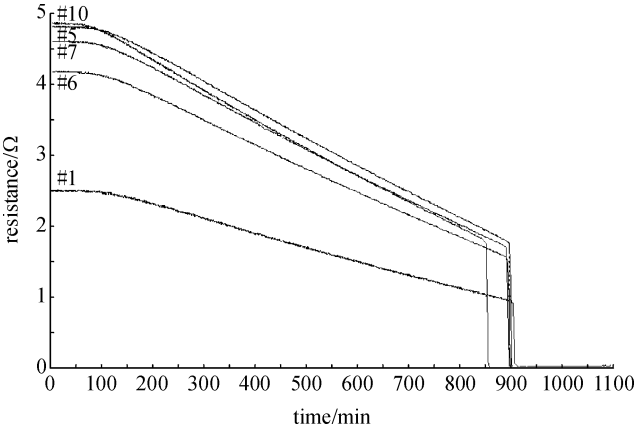

Fig. 4 Electric resistance of superconducting coils in cooldown course

I_c measurement: when the temperature of the magnet is between 13.5 K and 19 K, we apply AC voltages from 0 V to 500 V to measure the insulation against the earth and the inductance with voltages from 0 V to 50 V. Both of the currents are less than 100 mA. In the course of measurement, the magnet temperature does not change despite the existence of resistance.

In the experiment, the DC current is increased manually. At the time of 95th and 118th seconds, current and voltage peaks appear respectively (shown as Fig. 5). The variety of temperature is monitored and recorded in the I_c measurement. Figures 6 and 7 show the upside and the underside temperature variations of the magnet in one data acquisition cycle.

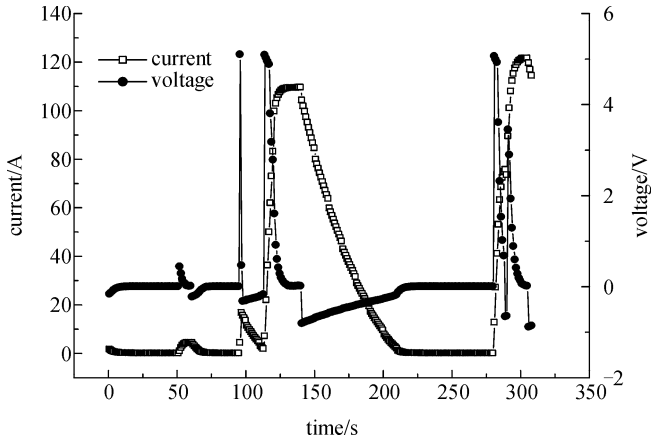

Fig. 5 Voltage and current in I_c measurement

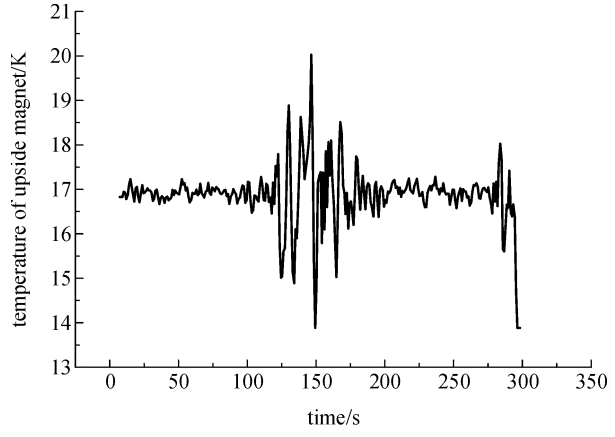

Fig. 6 Temperature of magnet upside during I_c measurement

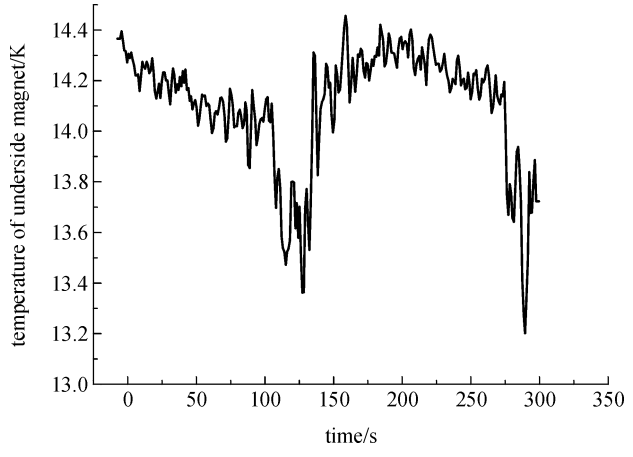

Fig. 7 Temperature of magnet underside during I_c measurement

During the magnetic energy excitation or release, the temperature of the magnet will rise. The temperature of the upside magnet reaches its maximum around 19.1 K at the 140th second while the average value is 17 K approximately. The temperature of the underside magnet reaches its maximum around 14.5 K at the 175th second, and the average temperature is about 14.2 K. The temperature of the upside magnet is high and the temperature rise is sharp because of the long distance to the cooling head. The underside magnet is well cooled because of the short distance to the cooling head with slight temperature rise. When the DC current reaches 140 A, the corresponding magnetic field is 4.5 T. The stored magnetic energy $W = LI^2/2 > 73.5$ kJ. When the DC current reaches 150 A, the magnet is quenched and its top part temperature reaches 27.3 K.

AC loading experiment of the SMES and results analysis: the dynamic characteristic experiment is carried out by applying a multi-module converter to charge and discharge the magnet [7]. In the converter DC side, certain AC harmonics exist and the maximal frequency is about 2 kHz. Hence, the magnet undergoes alternating magnetic fields in the course of the dynamic experiment and its temperature will definitely rise.

The temperature field of the magnet was simulated by finite element method (FEM) before the experiment. The average temperature value of the magnet was around 26 K with numerical simulation method during the current loading experiment [8].

When the magnet runs under 18 K, the maximal loading current is about 60 A. The speed of excitation is 1 A/s; the frequency is around 1 kHz and the voltage is 100 V. The temperature diversifications of the magnet within one data acquisition circle are displayed in Fig. 8. The curves #1 and #2 are the temperatures of the underside and upside magnet, respectively. The curve #3 is the cooling head temperature of the G-M cryocooler B. The experiment data show that the temperature of the upside magnet reaches its maximum at 32 K approximately at the 650th second and the average temperature is about 26.3 K. The temperature of the underside parts achieves its maximum at about 26 K and the average temperature is about 25.1 K, which means that the axial temperature difference is around 1.2 K.

The comparison of the two experiments indicates that: in DC current loading, the temperature rise is insignificant under relatively large current value; in contrast, for the dynamic current-loading case, this temperature change is considerably larger and sharper even under a relatively lower operating current, as long as the frequency is high. We attribute this difference to the following reasons: in the current-loading experiments, large AC loss means more heat generated in the dynamic loading process. During the DC current loading experiment and dynamic simulation experiment, the conducting frames could transport the heat load to the G-M cryocoolers timely when the AC loss is little. Also the cryogenic system can ensure magnet to run less than T_c when the operating current is within AC 60 A in the dynamic experiment. The application of flexible conducting components and inner conduction canister is helpful to equalize the temperature of the magnet in the current loading experiment [9].

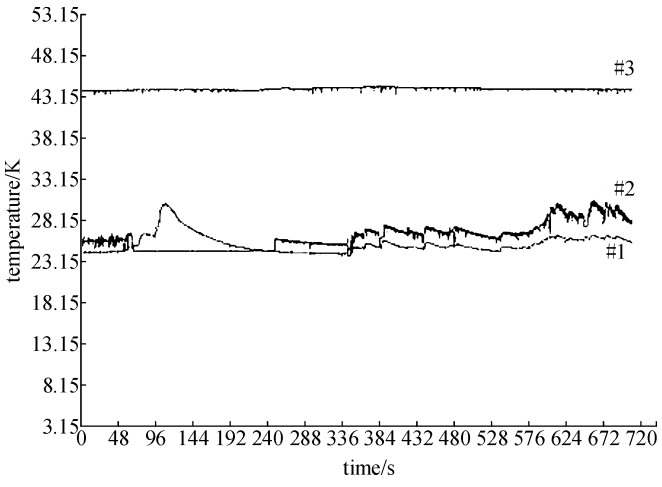

Fig. 8 Temperatures of magnet upside and underside during dynamic current loading

5 Conclusions

The experiments have demonstrated that the application of a flexible conducting frame, conducting poles, conducting board and inside conducting canister are effective in decreasing magnet temperature immediately and equalizing its temperature. Meanwhile, a relatively large axial temperature difference is generated by the long distance from the magnet upside to the refrigerator head, which also makes the temperature of the magnet upside rise sharply and has high average temperature.

According to Eqs. (1), (2), (4) and the experiment results, heat transfer effectiveness of SMES cryogenics system could be improved further by reducing the current ramp speed of the magnet, increasing the heat transfer coefficient of the conduction cooling structure and decreasing the shield temperature.

The optimization of heat transfer of the key part is extremely significant in the cryogenic system of SMES device and should be well considered.

Acknowledgements This work was supported by the Hi-Tech Research and Development Program of China (No. 2002AA306331-4), the National Natural Science Foundation of China (Grant No. 51076013), the Research Fund for the Doctoral Program of Higher Education of China (No. 200040487039).

References

1. Wang H L, Rao R S, Li J D, Tang Y J, Cheng S J, Pan Y. Progress on cryogenic technology applied in superconducting electric engineering. Automation of Electric Power Systems, 2001, 25(17): 65–68 (in Chinese)
2. Liu Z H. AC Loss and Stability of Superconducting Magnet. Beijing: National Defense Industry Press, 1992, 83 (in Chinese)
3. Tasaki K, Ono M, kuriyama T. Study on AC losses of a conductive cooled HTS coil. IEEE Transactions on Applied Superconductivity, 2003, 13(2): 1565–1568
4. Wang J X. Superconducting Magnet. Beijing: Atomic Energy Press, 2003, 150 (in Chinese)
5. Brechna H. Superconducting Magnet Systems (in Chinese, trans. Jin Dechang). Beijing: Science Press, 1986
6. Dresner L. Quench energies of uncooled superconductors. Cryogenics, 1994, 34(1): 77–82
7. Li J, Xu D H, Cheng K W E, Tang Y J. Carrier-swapping method to equalize current in a multi-modular current source converter for SMES. Proceedings of the CSEE, 2004, 24(7): 106–111 (in Chinese)
8. Wu G, Wang H L, Tang S M. Temperature field simulation and experiment research for 35 kJ HTS magnet of superconducting magnetic energy storage (SMES). In: Proceedings of 2006 Conference of Refrigeration and Cryogenics Engineering, 2006, 10
9. Wang H L, Wu G. A conduction cooling device application to HTS magnet. China Patent, CN2731650, 2005-10-05